Check for updates

Effects of riboflavin and AQS as electron shuttles on U(VI) reduction and precipitation by *Shewanella putrefaciens*

Pingping Wang, [ID] [ab] Faqin Dong,*[ab] Xuhui Wang,[c] Mingxue Liu, [ID] [a] Xiaoqin Nie,[a] Lei Zhou,[ab] Tingting Huo,[ab] Wei Zhang[a] and Hongfu Wei[c]

Understanding the mechanisms for electron shuttles (ESs) in microbial extracellular electron transfer (EET) is important in biogeochemical cycles, bioremediation applications, as well as bioenergy strategies. In this work, we adapted electrochemical techniques to probe electrochemically active and redox-active *Shewanella putrefaciens*. This approach detected flavins and humic-like substances of *Shewanella putrefaciens*, which were involved in electron transfer to the electrode. A combination of three-dimensional excitation-emission (EEM) florescence spectroscopy methods identified a mixture of riboflavin and humic-like substances in supernatants during sustained incubations. The reductive behaviour of U(VI) by *Shewanella putrefaciens* in the presence of riboflavin (RF) and anthraquinone-2-sulfonate (AQS) was also investigated in this study. The results indicated that RF and AQS significantly accelerated electron transfer from cells to U(VI), thus enhancing reductive U(VI). The precipitate was further evidenced by SEM, FTIR, XPS and XRD, which demonstrated that chernikovite [$H_2(UO_2)_2(PO_4)_2 \cdot 8H_2O$] became the main product on the cell surface of *S. putrefaciens*. In a contrast, U(IV) mainly existed amorphously on the cell surface of *S. putrefaciens* with added RF and AQS. This work has significant implications in elucidating RF and AQS as electron shuttles that are efficient in reduction of uranium in geological environments.

1. Introduction

Environmental contamination by uranium is mainly produced by mining, milling and the disposal of uranium waste, which causes a wide range of environmental pollution and induces a serious threat to human health.[1,2] Traditional processing methods such as chemical precipitation,[3] ion exchange,[4] and evaporation concentration[5] can effectively prevent the pollution of U(VI) in contaminative environments, but these methods generate secondary pollution, incur high production costs, and require harsh processing. The bioreduction of U(VI) has been studied in terms of microbial reduction of soluble U(VI) to insoluble U(IV), which provides an alternative approach that has been considered to be one of the prominent remediation strategies for U-contaminated sites.

Dissimilatory metal reducing bacteria (DMRB) can directly reduce soluble U(VI) to insoluble U(IV).[6–8] *Shewanella putrefaciens*

(*S. putrefaciens*), is a facultatively anaerobic bacteria, which has primarily been used to accumulate and immobilize uranium in the bioremediation of uranium-contaminated wastewater. Recent studies have indicated that *S. putrefaciens* has attracted much attention in the reductive bioremediation of U(VI), Cr(VI) and organic pollutants.[9,10] Some microbes which were also reported can accumuled and immobilize uranium *via* the biomineralization process, precipitating uranium through complexation with anions.[11,12] Extracellular electron transfer (EET) is one of the most fundamental life processes, which the exchange of information and energy with other microorganisms or with their external environments. Direct EET, conductive nanowires, and electron shuttles-mediated EET have been identified as main mechanism of EET.[13] Many researchers have used various electron shuttles, such as: melanin, phenazine derivatives, flavins, and humic substances (HS) to enhance U(VI) bioreduction.[14,15]

Quinones are a redox active group of humic substances widely present in soil, water and even activated sludge, and can act as electron shuttles facilitating the reduction of extracellular electron acceptors and the degradation of pollutants.[16] AQS a synthetic quinone that has been used extensively as a model for the redox properties of quinone groups in HS, enhance the reduction of iron oxides by DIRB.[17] Research has also shown that humic acid acting as a medium for electronic

[a]*The Key Laboratory of Solid Waste Treatment and Resource, Ministry of Education, Southwest University of Science and Technology, Mianyang, Sichuan, 621010, China. E-mail: fqdong@swust.edu.cn; Tel: +86-0816-6089-013*

[b]*School of Environment and Resource, Southwest University of Science and Technology, Mianyang, Sichuan, 621010, China*

[c]*School of Life Science and Engineering, Southwest University of Science and Technology, Mianyang, Sichuan, 621010, China*

transformation can effectively promote U(VI) reduction under experimental conditions with the coexistence of humic reductive bacteria and humic acid.[18]

Flavins, a group of redox-active compounds, are found in most microorganisms. The flavins present in *Shewanella oneidensis* account for 75% of the EET capacity. A study on the electron transfer pathway for U(VI) reduction mediated by flavin, which is secreted by the *Shewanella* species, demonstrated that flavin may also act as a mediator during the reduction of U(VI) to U(IV), accelerating its reduction.[19] Although the reduction rates of these contaminant metals could be enhanced in the presence of flavins and humic substances, few studies are available on the biomineralization of uranium with added electron shuttles by *S. putrefaciens*.

In this work, *S. putrefaciens* was used as model bacterium. The aims of this study are to indentify *S. putrefaciens* that are electrochemically active and mediate EET *via* self-secreted flavins. Interface interaction between uranium ions and *S. putrefaciens* cell with ESs was investigated, followed by spectroscopic and mesoscopic analyses. An interface interaction mechanism of bioreduction between *S. putrefaciens* and uranium was identified *via* a combination of scanning electron microscope (SEM), Fourier transform infrared spectroscopy (FTIR), X-ray photoelectron spectroscopy (XPS), and X-ray diffraction (XRD) technique. This paper highlights that flavins and quinones are ubiquitous mediators for microorganism EET and will play an important role in the application of microorganisms in geochemical mineral cycling and bioelectrochemical systems.

2. Material and methods

2.1 Material and bacteria cultivation

S. putrefaciens was isolated from a potential disposal site of low uraniferous radioactive waste in Southwest China. LB (Y-) medium consisting of yeast extract (5 g L^{-1}, Sangon, China), NaCl (5 g L^{-1}), peptone (10 g L^{-1}, Sangon), and agar (20 g L^{-1}) was used to cultivate the *S. putrefaciens*. The microorganisms were incubated in a bed temperature incubator at 200 rpm for 16 h. The cultures were then washed twice with sterile saline solution (0.9% NaCl) and resuspended in 50 mL sterilized saline solution with a cell density of $\sim 2 \times 10^9$ colony forming unit per millilitre (cfu mL^{-1}). The U(VI) stock solution (1.0 g L^{-1}) was prepared from UO$_2$(NO$_3$)$_2$·6H$_2$O in a 0.01 M HNO$_3$ solution. The reagents were purchased as analytical grade and used without further purification.

2.2 Microbial reduction of U(VI) experiments

Kinetic experiments of U(VI) reduction were conducted in 100 mL serum bottles containing 50 mL of LB medium with 15 mM acetate and different AQS and RF values (0.5, 1.0, 1.5 mM) as the electron donor and electron shuttle, respectively. All media were buffered by bicarbonate solutions (pH = 5.0) and autoclaved at 121 °C for 20 min prior to use. The U(VI) stock solution was sterilized by filtration at 0.22 μm and spiked into the media to give a final concentration of 100 mg L^{-1}. After the

media was purged with N$_2$/CO$_2$ (80% : 20%) for 30 min, *S. putrefaciens* were inoculated into the media (approximately 0.9 × 10^{10} cells per L) and the reactors were tightly sealed with rubber stoppers and aluminium caps. Each experiment was performed in triplicate under identical conditions in an incubator at 30 °C.

The concentrations of U(VI) in supernatant were determined using the spectrophotometrically Arsenazo III method at a wavelength of 652 nm.[20] Removal percentage (*R*) could be expressed as eqn (1).

$$R = \frac{c_0 - c_t}{c_0} \times 100\% \tag{1}$$

C_0 and C_t are the initial and the equilibrium concentrations of U(VI) in the solution respectively.

2.3 Electrochemical analysis

The photoelectrochemical measurement was performed in a conventional three-electrode system linked with the electrochemical workstation (Princeton Applied Research, USA, model PARSTAT 4000). An FTO, a platinum wire, and a saturated calomel electrode were used as the working electrode, counter electrode and reference electrode, respectively. The electrolyte used was aqueous phosphate-buffered solution (PBS, 50 mM, pH = 5.0). To clarify if the redox peaks originated from the reaction of compounds in the supernatant, the culture supernatant was collected for subsequent cyclic voltammetry (CV) and differential pulse voltammetry (DPV). As a control experiment, pure riboflavin (Sinopharm, China) was dissolved in the PBS and studied using CV. The CV scan rate used was 50 mV s^{-1}. For DPV studying the oxidation reactions, the staircase was 0.004 V, the initial potential was 0 V, and the final potential was −1 V.

2.4 EEM, SEM, FTIR, XPS and XRD analysis

EEMs of samples were recorded at room temperature with a 700 V Xe lamp and a 1 cm quartz cell (F-7000, Hitachi, Japan). The EEM spectra were recorded at excitation (E_x) wavelengths of 200–450 nm and emission (E_m) wavelengths of 250–600 nm with 5 nm and 1 nm resolution, respectively. The slit width for excitation and emission were both set to 5 nm. SEM-EDS were examined on Ultra 55 SEM coupled with Oxford IE450X-Max80 EDS successively. The samples were prepared by fixing contrast and U(VI)-loaded *S. putrefaciens* with 2.5% glutaraldehyde solution on glass flake for 12 h. Then, the samples were dehydrated in a graded ethanol series according to the sequence of 30%, 50%, 70%, 90%, and 100%. After air-dried and gold-sputtering for 150 s, samples were analysed by an SEM instrument. For EDS analysis, the electron beam was ejected vertically in the horizontal placement of the sample plane at an accelerating voltage of 15 keV and magnification of 9000 times. FTIR spectra were collected from a PerkinElmer Nicolet-5700 spectrophotometer in the wave number range of 400–4000 cm^{-1} at room temperature. Bacteria before and after U(VI) sorption were obtained for FTIR analysis after mixing with KBr in ratio of 1 : 100. A Thermo Escalab 250 XPS was conducted at 150 W with Al Kα

radiation. The XPS data were processed using the XPSPEAK software (version 4.1). The XRD analysis was recorded by a PANalytical X'Pert PRO diffractometer with Cu-Kα radiation (k = 1.5406 Å). The voltage and electric current was 40 kV and 40 mA, respectively. The data were analysed using the X'Pert High Score Plus software.

3. Results and discussion

3.1 Evidence for a redox mediator involved in electron transfer

Flavins are reported as components of yeast extract and mediate electron transfer between an electrode and bacteria.[21] The major features of the CVs of *S. putrefaciens* are shown in Fig. 1a. An obvious oxidation peak at −0.30 V (*vs.* SCE) and reduction peak at −0.58 V (*vs.* SCE) appeared in the CVs of *S. putrefaciens*, indicating that the flavins in *S. putrefaciens* are capable of reversibly accepting and donating electrons. Marsili *et al.* (2008) summarized that *S. oneidensis* MR-1 secretes flavins to mediate EET between the cells and an electrode: the formal potential of flavins is −0.41 V (*vs.* SHE).[22] A similar conclusion was found of *P. stipitis*, *Bacillus* and *Pichia*, which have riboflavin excretion system.[14,21]

DPV can detect lower concentrations of redox compounds by optimization of faradaic and capacitive currents. As shown in Fig. 1b, the pair with the peak potentials, E_p = −0.58 V (*vs.* SCE) (anodic) and −0.4 V (*vs.* SCE) (cathodic) appeared, which approximate the redox potential of pure riboflavin. In the *S.*

putrefaciens culture supernatants, the pair of DPV peaks with anodic peaks at E_p = −0.52 V and cathodic peaks at E_p = −0.42 V. It has been reported that some bacteria can liberate flavins and c-type cytochromes to outside of cells.[23] The CV of riboflavin are shown in Fig. 1c, in which oxidation peak at −0.29 V (*vs.* SCE) and reduction peak at −0.60 V (*vs.* SCE). These observations were consistent with peaks of *S. putrefaciens*. Therefore, we hypothesize that the redox peaks in the CV and DPV provide indications that *S. putrefaciens* may yield flavins.

3.2 Characterizations of *S. putrefaciens*

Three-dimensional fluorescence spectra for a component of *S. putrefaciens* that was extracellularly secreted are shown in Fig. 2. These fluorescence peaks correspond to proteins and soluble microbial metabolites. As shown in Fig. 2a, one main peak was observed from the three-dimensional fluorescence spectra of *S. putrefaciens* in the 12 h culture. The peak was identified at excitation/emission (E_x/E_m) wavelengths of 330/400 nm. After the 24 h and 48 h culture, the peak intensity was increased, and the peak position does not change (Fig. 2b and c). According to previous reports, the peaks were assigned to protein-like substances and humic-like substances.[24-26] After adding RF, the fluorescent intensity of the peak decreased in 12 h (Fig. 2d). The addition of RF reacts directly with uranium, reducing the toxicity of uranium on microorganisms, while altering the metabolites of microorganisms. After 24 h and 48 h culture, the peak intensity was increased, which indicates that microorganisms react with uranium by secreting humic-like substances
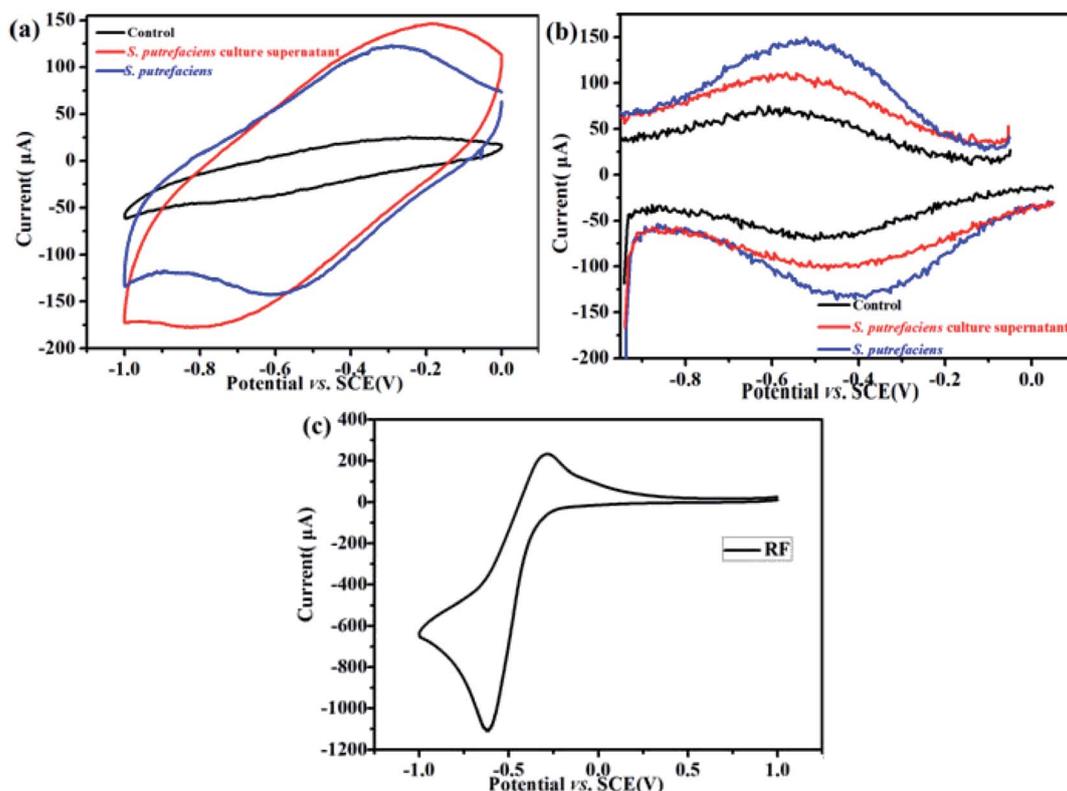

Fig. 1 CVs of *S. putrefaciens* in the culture medium supernatants and the control in 0.05 M PBS; the corresponding DPV assays (b). CV of riboflavin in 0.05 M PBS (c). Tests were repeated more than 3 times under a N₂ environment at a scan rate of 50 mV s⁻¹.

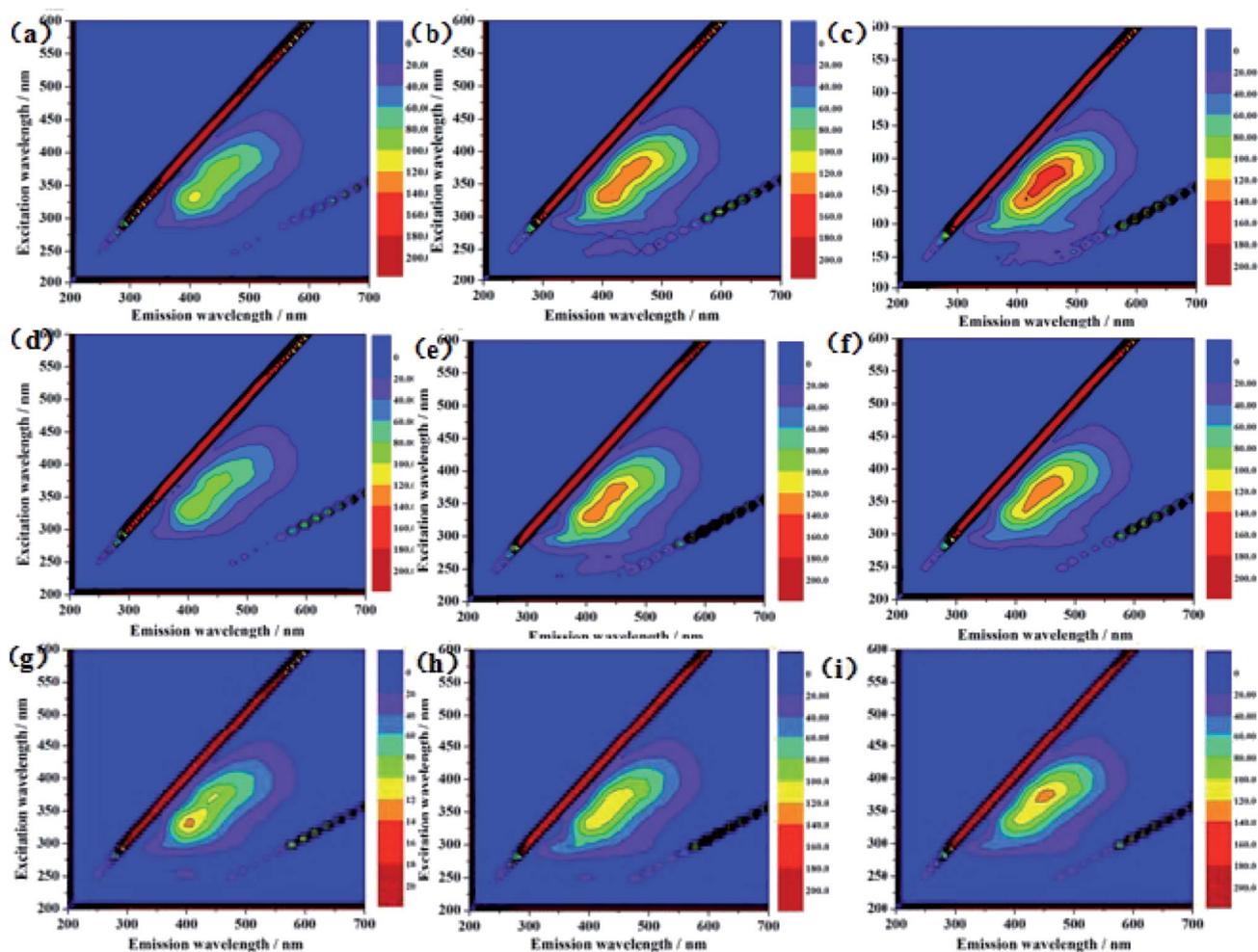**Fig. 2** Three-dimensional excitation-emission matrix (E_X, E_M) fluorescence spectroscopy of U-loaded *S. putrefaciens* 12 h (a), 24 h (b), 48 h (c), RF-U(VI)-*S. putrefaciens* 12 h (d), 24 h (e), 48 h (f), and RF-U(VI)-*S. putrefaciens* 12 h (g), 24 h (h), 48 h (i).

(Fig. 2e and f). After adding AQS, which affects the fluorescence intensity of humic-like substances, the fluorescent intensity of the peak increased in 12 h (Fig. 2g). The humic concentrations of microbial metabolites were reduced compared with controls after the 24 h and 48 h culture (Fig. 2h and i). The result reveals that *S. putrefaciens* can release little amounts of humic-like substances to outside cells, and the added AQS rapidly react with U(VI).[27]

3.3 Effects of RF and AQS on U(VI) reduction

The effect of RF and AQS addition on the reduction of U(VI) by *S. putrefaciens* was presented in Fig. 3. While in the presence of AQS, the initial reduction rates were higher than that without AQS (Fig. 3a). 40% and 75% of U(VI) was removed from the medium with the addition of 0 and 1.5 mM AQS, respectively (pH = 5.0, $C_{U(VI)}$ = 100 mg L^{-1}). When the AQS concentration increased, the adsorption efficiency increased slowly for the *S. putrefaciens* cells. These observations confirm that humic substances could play a significant role in enhancing the bio-reduction of U(VI), perhaps by acting as electron shuttles or mediators between U(VI) and microbes. Similarly, other investigators reported that humic substances could enhance the

electron-transfer reactions and bioreduction of Fe(III) or iron oxides by a variety of microorganisms.[28,29]

RF, the primary secreted flavin, was tested to assess its effect on U(VI) reduction. Fig. 3b shows that U(VI) reduction was accelerated and positively correlated while in the presence of riboflavin. When the RF concentration increased from 0 to 1.5 mM, the removal rate efficiency raised from 40% to 65% for *S. putrefaciens* (pH = 5.0, $C_{U(VI)}$ = 100 mg L^{-1}), respectively. The electron transfer rate from *S. putrefaciens* to electron acceptor has accelerated, which fits the definition of an endogenously produced mediator. Similarly, bacteria, yeast, and plants use the combined abilities of flavins in metal acquisition.[30–32] Thus, our results indicate that self-secreted riboflavins might be helpful and contribute to U(VI) reduction in environments.

3.4 Analysis of uranium speciation

3.4.1. SEM and EDX analysis. To explore the surface interactions between uranium and *S. putrefaciens*, the characteristic of uranium deposition was determined by SEM coupled with EDS. Fig. 4 shows the SEM images of *S. putrefaciens* with and without electron shuttles exposure to 100 mg L^{-1} of uranium for 20 hours. The original *S. putrefaciens* exhibited an
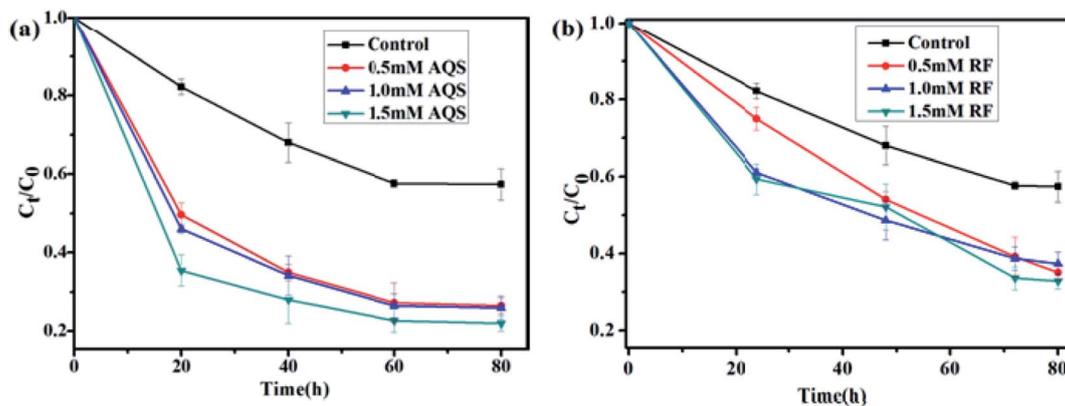
Fig. 3 Effect of AQS concentration (a) and RF concentration (b) on reduction of U(VI) by *S. putrefaciens* at pH 5.0, $C_{U(VI)} = 100$ mg L^{-1}.

intact shape and smooth surface (Fig. 4(a and b)). After incubation with U(VI) solutions, a large number of lamellate precipitates developed on the surface of the living bacteria (Fig. 4(c and d)). The EDS spectra derived from the cluster crystal exhibited distinct U and P and O peaks, which evidence the formation of uranium phosphate minerals. Wang *et al.* (2017) found similar precipitation on the root cells of *Saccharomyces cerevisiae* after U(VI) sorption.[33] Uranium precipitates occurred due to phosphate release from the cellular polyphosphate, likely as a response of cells to added uranium.[21,34] By comparison, only small similar precipitants were observed on the surface of *S. putrefaciens*, when AQS (Fig. 4(e and f)) and RF (Fig. 4(g and h)) are added to 100 mg L^{-1} U(VI) solutions. The EDS spectrum derived from the lamellar precipitation exhibited obvious U and P peaks. The results indicated that AQS and RF were found to greatly increase the bioreduction rates of U(VI), when humics were present during the bioreduction process.[29] However, our observations imply that the precipitates of U(IV) were reduced on the cell surface. The results is supported by the XRD images in Fig. 7 showing the formation of non-uraninite U(IV) at 20 h.

3.4.2. FTIR spectroscopy. The FTIR spectra of U(VI) reduction with and without added electron shuttles by *S. putrefaciens* are shown in Fig. 5. After being loaded with uranium, very obscure bands at 3392.3 cm^{-1} indicated the presence of both amine (*n*N–H) and bonded hydroxyl (*n*O–H) groups,[35] which are no obvious changes. The peak at 1636.9 cm^{-1} corresponds to stretching of amide I blueshifed by 7 cm^{-1}. Compared with FTIR spectrum of *S. putrefaciens* cells, the peaks at 1546.9 cm^{-1} and 1384 cm^{-1}, corresponding to amide II, and amide III bands, appeared after uranium biosorption.[36] An obscure band is observed at 1079.0 cm^{-1}, which is attributed to the vibration of the phosphodiester group [*vs.* (–PO$_2^-$)].[37] The band of U(VI)-loaded *S. putrefaciens* showed blueshifed by 54 cm^{-1} in comparison to the bands of original cells, suggesting an important role of phosphates groups in the immobilization of U(VI). Previous research reported that phosphate groups were conductive to cationic binding and might serve as nucleation sites for further large amounts of metal deposits.[20,24,35] The different peak shapes were also observed in the fingerprint region. Previous research illustrated the asymmetric stretching

frequencies of UO$_2^{2+}$ around ranges between 950 and 890 cm^{-1}.[38] A new characteristic peak at 919 cm^{-1} was observed after U(VI) treatment, representing a mix of monomeric, polymeric or carbonate containing hydroxyl U(VI) complexes.[39]

The FTIR spectrum of *S. putrefaciens* with added AQS (Fig. 5) showed that the amide I redshifted by 9 cm^{-1}, which is consistent with original *S. putrefaciens*. The peak at 1546.9 cm^{-1} and 1384 cm^{-1}, corresponding to amide II, and amide III bands, also appeared with added AQS. The FTIR spectra of tetravalent and hexavalent uranium presented a characteristic peak between 400 and 620 cm^{-1} and 800–1100 cm^{-1}, respectively.[22] Interestingly, the peak at 474.9 cm^{-1} were observed, suggesting that the U(IV) surface species was formed at in the presence of AQS.[40] However, no hexavalent uranium peak was observed, which might have resulted from the less immobilized U(VI) amounts. The FTIR spectrum of *S. putrefaciens* with added RF showed that similar variety of *S. putrefaciens*. The intense band is observed in 472.3 cm^{-1}, which also comes from stretching the vibration of U(IV). Therefore, RF and AQS thus mediate the interaction of microorganisms and U(VI), which increase microbial reduction of U(VI).

3.4.3. XPS analysis. To explore the interactions between uranium and *S. putrefaciens* on cell surface, the uranium deposition was analysed by XPS. Fig. 6a shows the full spectrum of the X-ray photoelectron binding energy curves of *S. putrefaciens* with and without added electron shuttles. It must be noted that the N 1s, P 2p and U 4f peaks were very weak due to their low composition. After a uranium-loaded sample, the most intense peaks of U 4f (Fig. 6b) were recorded at approximately 382.0 and 392.8 eV, which were correspond to the spin–orbit (L–S) split U 4f$_{7/2}$ and U 4f$_{5/2}$ states, respectively.[41] The results from XPS suggest that the uranium reaction product is most likely a U(VI) oxidation state. The low intensity peaks at approximately 388 and 400 eV could be shake-up satellites, which occur as a consequence of the change in electrostatic potential during the photoelectron excitation process.[42] This is applicable for both U 4f$_{7/2}$ and U 4f$_{5/2}$ states. Similar observations were made by Liu *et al.* (2010).[38]

After the AQS-added sample (Fig. 6c), the relative intensity of U 4f$_{7/2}$ of U(IV) greatly changed and the positions of the peaks were slightly shifted. The satellite peak observed at
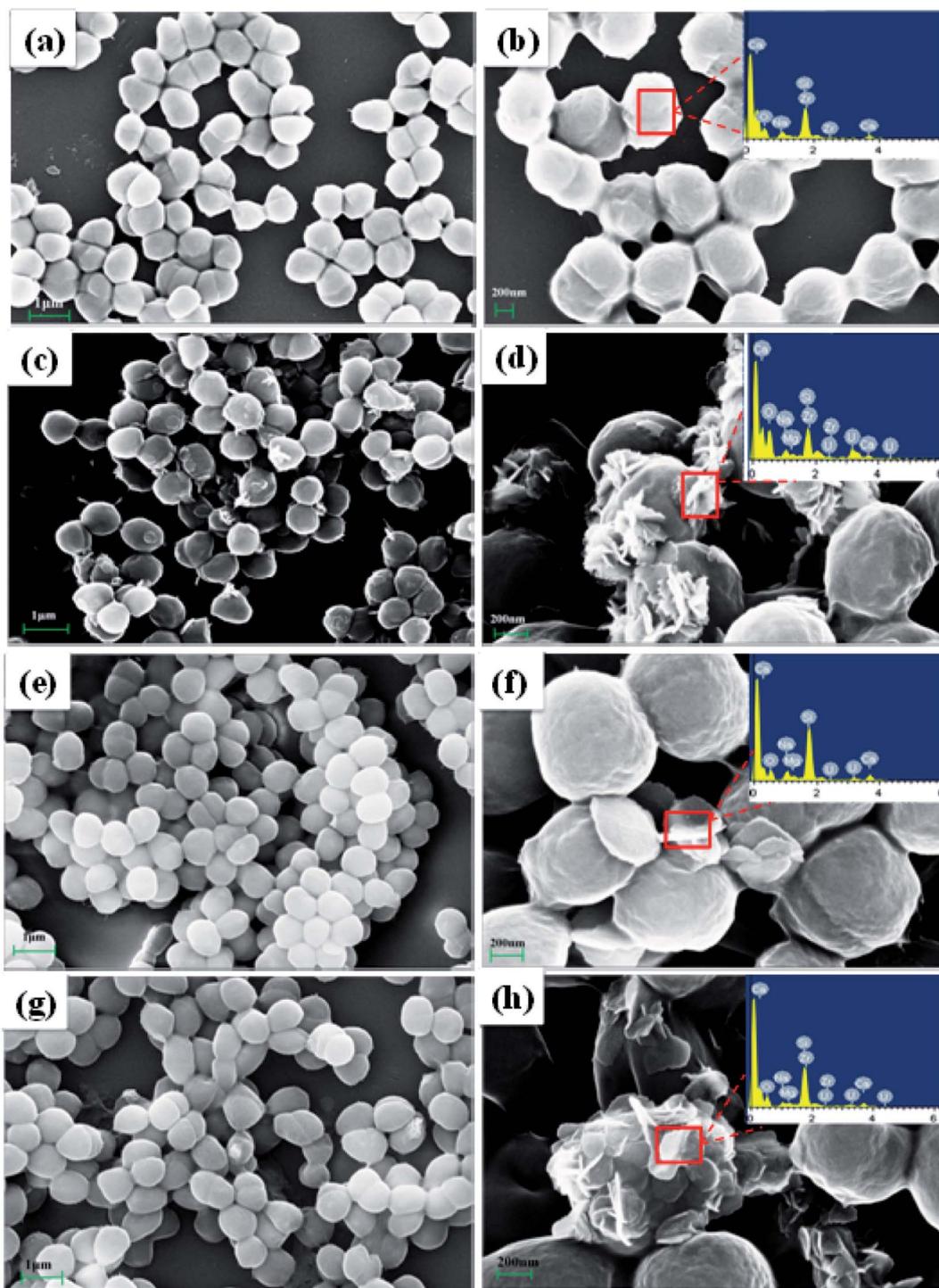
Fig. 4 SEM images of original *S. putrefaciens* (a and b), uranium-loaded *S. putrefaciens*. (c and d), AQS- U(VI)-*S. putrefaciens* (e and f) and RF-U(VI)-*S. putrefaciens* (g and h), $C_{U(VI)} = 100$ mg L^{-1}.

397.0 eV, 397.6 eV which are approximately 7 eV from the U 4f$_{5/2}$ peak, may be attributed to a shake-up transition from the oxygen-derived 2p band to the U (5f) Fermi level of UO$_2$.[43,44] As shown in Fig. 6d, the binding energy of U 4f$_{7/2}$ and U 4f$_{7/2}$ of U(IV) had shifted slightly with added RF, which indicated that the compounds on the cell surface were changed after interaction with uranyl ions.

3.4.4. XRD analysis. Investigating the structural stability of uranium speciation on the *S. putrefaciens* is necessary to understand the fate and transport of uranium in real environments. Fig. 7 shows the XRD pattern of uranium-loaded *S. putrefaciens* with and without added AQS/RF at pH 5.0. A broad peak approximately $2\theta = 20°$ on the control sample indicated the pure *S. putrefaciens* was amorphous. After uranium
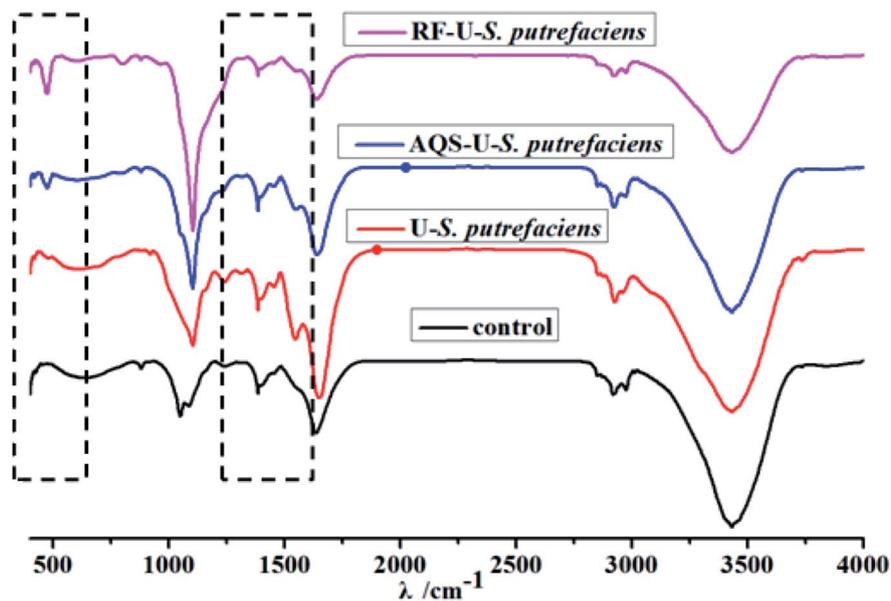
Fig. 5 FTIR spectra of U(VI) reduction with and without added electron shuttles by *S. putrefaciens* at pH 5.0, $C_{U(VI)}$ = 100 mg L^{-1}.

exposure, obvious diffraction peaks were observed, which identified as chernikovite [$H_2(UO_2)_2(PO_4)_2 \cdot 8H_2O$] (PDF-2 00-008-0296). The same results were also observed by Nie *et al.* (2017) and Huang *et al.* (2017), in which bacterial phosphatase activity cleaves organophosphates, liberating inorganic phosphate that precipitates with aqueous U(VI) as uranyl phosphate minerals.[20,24] The results indicated that *S. putrefaciens* could

form nano-crystalline uranium precipitate, and the possible complexes of uranium with phosphate would facilitate uranium precipitation.[21,39] However, no crystallized uranium product was observed on addition RF and AQS in uranium, which might be attributed to the low content of U(IV) (*i.e.*, <5% wt%) or the formation of monomeric or nonuraninite U(IV) which lacks the crystalline structure of uraninite.
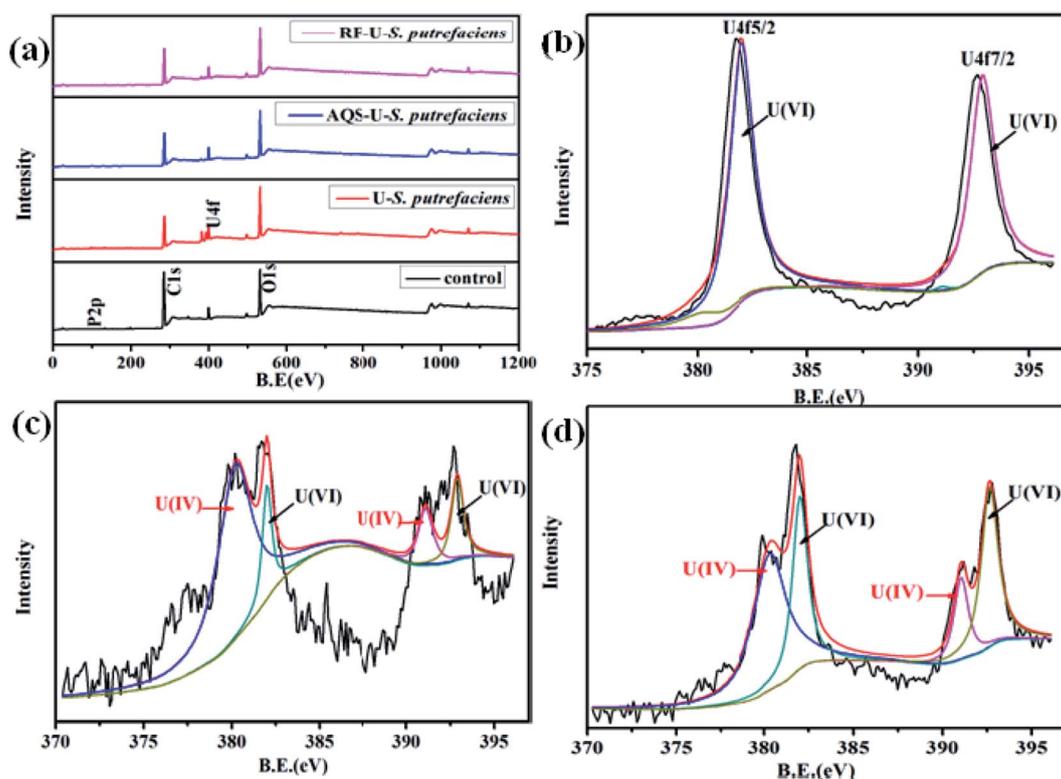

Fig. 6 The survey scans of XPS spectra of U(VI) reduction, with and without added RF/AQS, by *S. putrefaciens* cells at pH 5.0: total survey scans (a), U 4f spectra of U-loaded *S. putrefaciens* (b), U 4f spectra of AQS-U(VI)-*S. putrefaciens* (c), and U 4f spectra of RF-U(VI)-*S. putrefaciens* (d).
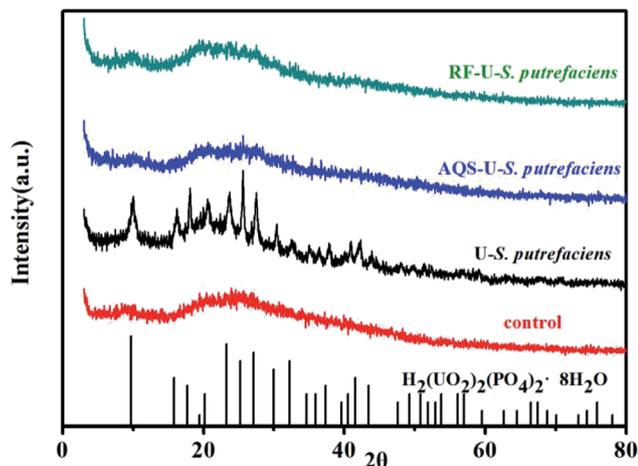
Fig. 7 XRD pattern of U(VI) reduction with and without added electron shuttles at pH 5.0, $C_{U(VI)} = 100$ mg L^{-1}.

3.5 The possible mechanisms of uranium reduction by *S. putrefaciens*

Microbial reduction of soluble U(VI) to insoluble U(IV) is an important promising technique for *in situ* bioremediation of uranium wastewater. The present work investigated the mechanism of uranium transformation from U(VI) into U(IV) minerals by *S. putrefaciens* under electron shuttles conditions. The results showed that RF and AQS could be electron shuttles to significantly accelerate the U(VI) reduction.

Based on the above results and other studies, we propose an interface interaction process for bioreduction of *S. putrefaciens* with and without electron shuttles in Fig. 8. For adsorption system of *S. putrefaciens*, first uranyl ions were attached on the cell surface *via* physical or chemical interactions (Fig. 8a). The cell surface was covered with a large number of functional groups, such as: hydroxyl, amide, and phosphate, which also played an important role for complexation between uranyl ions

and cells.[36] Then under the stimulation of uranyl ions, the cells released phosphate by a metabolism-dependent process. The phosphate reacted with surface-complexed U(VI) and formed the nucleation phase of chernikovite [$H_2(UO_2)_2(PO_4)_2 \cdot 8H_2O$] minerals under appropriate physical–chemical conditions.

Microorganisms and U(VI) interface interaction processes under electron shuttles conditions shows in Fig. 8b. Electron shuttling between microorganisms and U(VI) consists of two steps: (i) the biotic reduction of the dissolved electron shuttles, which can be microbially mediated. Several studies showed different electron shuttles that the reducing capacities were very similar by chemical reduction and microbial reduction.[45] (ii) Electron shuttling process is the transfer of electrons from reduced shuttles to the U(VI). This means that reduced electron shuttles can be reoxidized by transferring their electrons to U(VI), leading to an increase microbial reduction of U(VI).[46] Electron shuttles thus increases the number of microorganisms that reduce U(VI), thereby increasing the importance of U(VI) reduction in the environment.

4. Conclusions

The RF and AQS mediated reduction U(VI) of Gram positive *S. putrefaciens* were studied. Electrochemical results indicated that microorganisms exhibit electrochemical activity. Subsequent three-dimensional fluorescence spectra proved that flavins were secreted from *S. putrefaciens*, which contributed to the EET. RF and AQS could be electron shuttles to significantly accelerate the U(VI) reduction. Thus, the interaction between reduced electron shuttles and U(VI) can be regarded as a kind of extracellular electron transfer. Chernikovite [$H_2(UO_2)_2(PO_4)_2 \cdot 8H_2O$] significantly formed on the cell surface of *S. putrefaciens* after 20 hours of contact with U(VI). We primarily find that the sorption of U(VI) mediates the occurrence of uranium biominerals. In contrast, U(IV) mainly existed amorphously on the
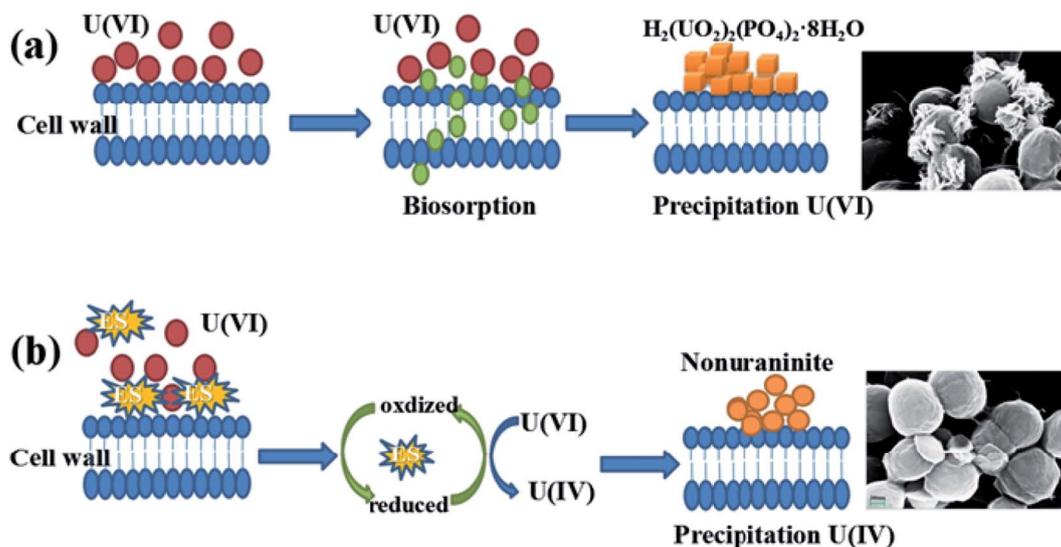

Fig. 8 A graphical analysis of the interface interaction process of *S. putrefaciens* towards uranium (a), interface interaction processes of U(VI) reduction with added electron shuttles (b).

cell surface of *S. putrefaciens* with added RF and AQS. In the process, electron shuttles can be used circularly, so a small quantity of electron shuttles would contribute notable action to the bacterial U(VI) reduction. Therefore, our work provided useful information on the mechanisms of uranium phase transform process with and without added ESs, including uranium bioreduction and phosphate biomineralization, which leads to a better understanding of the mechanisms governing uranium mobilization. These results will also be helpful to improve bioremediation technology of uranium wastewater.

Conflicts of interest

There are no conflicts to declare.

Acknowledgements

References

1 L. Newsome, K. Morris and J. R. Lloyd, *Chem. Geol.*, 2014, **363**, 164–184.

2 C. Ding, W. Cheng, Y. Sun and X. Wang, *Geochim. Cosmochim. Acta*, 2015, **165**, 86–107.

3 H. He, M. Zong and F. Dong, *J. Radioanal. Nucl. Chem.*, 2017, **313**, 59–67.

4 S. A. McMaster, R. Ram and S. Bhargava, *Miner. Eng.*, 2015, **81**, 58–70.

5 S. Abbasizadeh, A. R. Keshtkar and M. A. Mousavian, *Chem. Eng. J.*, 2013, **220**, 161–171.

6 D. R. Lovley, E. J. Phillips, Y. A. Gorby and E. R. Landa, *Nature*, 1991, **350**, 413.

7 D. R. Lovley and E. J. Phillips, *Appl. Environ. Microbiol.*, 1992, **58**, 850–856.

8 Y. Sun, X. Wang, Y. Ai, W. Huang and X. Wang, *Chem. Eng. J.*, 2017, **310**, 292–299.

9 F. Luan, W. D. Burgos, L. Xie and Q. Zhou, *Environ. Sci. Technol.*, 2009, **44**, 184–190.

10 M. E. Dollhopf, K. H. Nealson, D. M. Simon and G. W. Luther III, *Mar. Chem.*, 2009, **70**, 171–180.

11 A. J. Pinto, M. A. Goncalves, C. Prazeres, J. M. Astilleros and M. J. Batista, *Chem. Geol.*, 2012, **312–313**, 18–26.

12 X. Liang, L. Csetenyi and G. M. Gadd, *Appl. Microbiol. Biotechnol.*, 2016, **33**, 1–11.

13 L. Shi, H. Dong, G. Reguera and J. K. Fredrickson, *Nat. Rev. Microbiol.*, 2016, **14**, 651.

14 Y. Wu, T. Liu, X. Li and F. Li, *Environ. Sci. Technol.*, 2014, **48**, 9306–9314.

15 F. Khalili and G. Al-Banna, *J. Environ. Radioact.*, 2015, **146**, 16–26.

16 W. S. Ngah, S. Fatinathan and N. A. Yosop, *Desalination*, 2011, **272**, 293–300.

17 Y. Hong, P. Wu, J. Gu and S. Duan, *Appl. Microbiol. Biotechnol.*, 2012, **93**, 2661–2668.

18 J. X. Liu, S. B. Xie, Y. H. Wang and W. T. Wang, *Trans. Nonferrous Met. Soc. China*, 2015, **25**(12), 4144–4150.

19 S. Tsujimura, *Phys. Chem. Chem. Phys.*, 2010, **12**, 10081–10087.

20 W. Huang, X. Nie, F. Dong and S. Sun, *J. Radioanal. Nucl. Chem.*, 2017, **312**, 531–541.

21 C. A. Abbas and A. A. Sibirny, *Microbiol. Mol. Biol. Rev.*, 2011, **75**, 321–360.

22 E. Marsili, J. B. Rollefson, D. B. Baron, R. M. Hozalski and D. R. Bond, *Appl. Environ. Microbiol.*, 2008, **74**(23), 7329–7337.

23 A. Okamoto, K. Hashimoto, K. H. Nealson and R. Nakamura, *Proc. Natl. Acad. Sci. U. S. A.*, 2013, **110**(19), 7856–7861.

24 X. Nie, F. Dong and Z. Li, *ACS Sustainable Chem. Eng.*, 2017, **5**, 1494–1502.

25 Q. L. Fu, J. Z. He and D. M. Zhou, *Chemosphere*, 2016, **155**, 225–233.

26 W. Qiao, X. Wang and G. Chen, *Water*, 2017, **9**, 66.

27 Y. Wu, F. Li, T. Liu, R. Han and X. Luo, *Electrochim. Acta*, 2016, **213**, 408–415.

28 D. R. Lovley, *Nature*, 1996, **382**, 445–448.

29 L. Gu, B. Huang, C. Lai and X. Pan, *Sci. Total Environ.*, 2018, **631**, 641–648.

30 D. J. Worst, M. M. Gerrits and J. G. Kusters, *J. Bacteriol.*, 1998, **180**, 1473–1479.

31 A. Vorwieger, *Planta*, 2007, **226**, 147–158.

32 Y. R. Boretsky, *J. Basic Microbiol.*, 2007, **47**, 371–377.

33 T. Wang, X. Zheng, X. Wang and Y. Shen, *J. Environ. Radioact.*, 2017, **167**, 92–99.

34 E. Krawczyk-Barsch, L. Lutke, H. Moll and A. Rossberg, *Environ. Sci. Pollut. Res.*, 2015, **22**, 4555–4565.

35 R. C. Oliveira, P. Hammer, E. Guibal and O. Garcia, *Chem. Eng. J.*, 2014, **239**, 381–391.

36 M. Liu, F. Dong, W. Zhang and D. Wang, *RSC Adv.*, 2017, **7**, 50880–50888.

37 D. S. Alessi, J. S. Lezama-Pacheco and R. Bernier-Latmani, *Geochim. Cosmochim. Acta*, 2014, **131**, 115–127.

38 M. Liu, F. Dong and X. Pang, *Bioresour. Technol.*, 2010, **101**, 8573–8580.

39 E. Marsili, D. B. Baron, I. D. Shikhare and D. R. Bond, *Proc. Natl. Acad. Sci. U. S. A.*, 2008, **105**, 3968–3973.

40 X. Nie, F. Dong, N. Liu and J. Yang, *Appl. Surf. Sci.*, 2015, **347**, 122–130.

41 C. Ding, W. Cheng, Y. Sun and X. Wang, *Geochim. Cosmochim. Acta*, 2015, **165**, 86–107.

42 S. Bera, S. K Sali, S. Sampath and V. Venugopal, *J. Nucl. Mater.*, 1998, **255**, 26–33.

43 J. S. Lezama-Pacheco, J. M. Cerrato, H. Veeramani and J. R. Bargar, *Environ. Sci. Technol.*, 2015, **49**, 7340–7347.

44 S. Kushwaha, B. Sreedhar and P. Padmaja, *Langmuir*, 2012, **28**, 16038–16048.

45 E. D. Brutinel and J. A. Gralnick, *Appl. Microbiol. Biotechnol.*, 2012, **93**, 41–48.

46 X. Li, L. Liu and Y. Li, *Chemosphere*, 2013, **92**, 218–224.